Natural Resources Canada | Ressources naturelles Canada

GEOLOGICAL SURVEY OF CANADA
OPEN FILE 8820

Early Cambrian maximum depositional age for the upper Yelverton Formation, northern Ellesmere Island, Nunavut

T. Hadlari and W.A. Matthews

2021

Canada

GEOLOGICAL SURVEY OF CANADA
OPEN FILE 8820

Early Cambrian maximum depositional age for the upper Yelverton Formation, northern Ellesmere Island, Nunavut

T. Hadlari[1] and W.A. Matthews[2]

[1]Geological Survey of Canada, 3303 33rd Street Northwest, Calgary, Alberta
[2]Department of Geoscience, University of Calgary, 2500 University Drive Northwest, Calgary, Alberta

2021

Permanent link: https://doi.org/10.4095/328836

This publication is available for free download through GEOSCAN (https://geoscan.nrcan.gc.ca/).

Recommended citation
Hadlari, T. and Matthews, W.A., 2021. Early Cambrian maximum depositional age for the upper Yelverton Formation, northern Ellesmere Island, Nunavut; Geological Survey of Canada, Open File 8820, 15 p. https://doi.org/10.4095/328836

Publications in this series have not been edited; they are released as submitted by the author.

Abstract

U-Pb detrital zircon analysis of sandstone samples collected from northern Ellesmere Island during the summer of 2017 provides new depositional age constraints for the Yelverton Formation. Two samples from the same outcrop locality near the top of the formation have yielded an Early Cambrian maximum depositional age (MDA) of 532.1 ± 9.1 Ma. Because the overlying Grantland Formation contains late Early Cambrian trilobites (*Oldhamia*), we conclude that the uppermost Yelverton Formation is Early Cambrian. A near-depositional age fraction of detrital zircon is interpreted as a proxy for the age of igneous rocks within the Yelverton Formation, which is conservatively estimated as ranging from 551.1 ± 8.9 Ma to 532.1 ± 9.1 Ma.

Introduction

The Yelverton Formation represents the lowest and oldest part of the stratigraphy in the Hazen Trough portion of the Franklinian Basin (Trettin, 1998). Paleozoic strata of the Hazen Trough on northern Ellesmere Island where Paleozoic strata consist of deep marine facies that correlate to age-equivalent shallow marine strata of the Franklinian Shelf to the south (Trettin, 1994)(Figs. 1-2).

Distributed throughout parts of the Clements-Markham fold belt, the Yelverton Formation lies between rocks of Pearya terrane to the north and shallow marine deposits of the Franklinian Shelf to the south. Prior to this study, the only age constraint on the Yelverton Formation is that it is interpreted to be older than Early Cambrian (*Oldhamia*) trilobite fossils reported from the Grantland Formation (Trettin, 1994, 1998). Sandstone samples of the Yelverton Formation were collected during the summer of 2017, and U-Pb detrital zircon analysis was conducted at the University of Calgary to determine the sedimentary provenance and if possible to better constrain the depositional age.

Sample location

The sample locality is on the west side of a valley that extends southward from Kulutingwak Fiord (west of Yelverton Inlet shown in Fig. 1). The outcrop belt of the Yelverton Formation is contiguous with the outcrops at Yelverton Inlet. The stratigraphically lower boundary of the outcrop belt is marked by a thrust fault contact with the Yelverton Formation thrust over the Grantland Formation. In the approximate middle of the outcrop belt is a band of Carboniferous strata, which indicates that the exposed stratigraphic thickness of the Yelverton Formation has been structurally duplicated. Two samples were collected within 50 m of each other from the northern edge of the outcrop belt, within 100 m of the upper contact

with the overlying Carboniferous strata (Table 1). The samples are of fine-grained quartzose sandstone beds that are inter-stratified with fine-grained carbonate. Few sedimentary structures were observed but the depositional setting is probably similar to the rest of the Yelverton Formation, which consists mainly of deep marine carbonates interbedded with lesser mafic volcanic rocks, and intruded by mafic sills.

U-Pb detrital zircon: methodology

U-Pb isotopic data were collected at the Geo- and Thermochronology Laboratory at the University of Calgary. Detrital zircon populations in the Yelverton Formation samples were measured three times. The first ablation sequence used the large-n methodology (n = 300) outlined in Matthews and Guest (2017). Initial results were encouraging and identified a very small population of near-depositional age grains. To identify more of these grains, an additional round of large-n (n = 660) dating was conducted using methods modified after Daniels et al. (2017). Near-depositional age grains identified in the first two rounds were then re-ablated using a lower-uncertainty measurement method to provide better uncertainty for the MDA. Each method is described separately below.

Large-n (n = 300) Detrital Zircon Geochronology

Detrital zircons were separated using standard mineral separation techniques of crushing, milling, water tabling, heavy liquids and magnetic separation. A representative sample of the final zircon-rich separate was randomly selected and dump-mounted into a 12 x 15 mm Teflon™ form and cast in epoxy. Mounts were ground using 5 µm SiC film adhered to glass. Grinding continued until the surface reached roughly the midpoint of the smallest zircon population in the mount. Final polishing employed 3 and 1 µm diamond abrasive film adhered to glass. This polishing procedure ensured that all zircon populations in the sample were available for measurement and provided a very flat finish to ensure consistent laser focus.

U-Pb isotopic data were collected by laser ablation inductively coupled plasma mass spectrometry (LA-ICP-MS). Ablation occurred in a Laurin Technic™ M-50 two-volume ablation cell in an Applied Spectra Resolution 193 nm laser ablation system. To minimize signal wash-in and wash-out and maximize the efficiency of data acquisition no smoothing manifold was used. Samples were ablated for 15 s using a 22 µm beam diameter, a fluence of 2.1 J/cm^2 and repetition rate of 10 Hz. Each ablation was proceeded by an 8.5 s gas blank. These laser settings resulted in a ~17 µm deep pit. Additional information and performance metrics for the laser ablation system can be found in Müller et al. (2009). Isotopic signal intensities were measured using an Agilent 7700x quadrupole mass spectrometer.

Samples were measured using a sample-standard bracketing procedure. One measurement of the calibration reference material (FC1; 1099.9 Ma; Paces and Miller, 1997) was made between each 20 unknowns (approximately every 10 minutes). Eight measurements of SRM-NIST610 glass were used to calibrate U and Th concentrations. Zirconium was used to standardize these concentrations and assumed stochiometric abundance (49.7 wt%). Eight measurements of each of four validation reference materials (Table 2) were used to validate the results. A total of 300 unknowns were measured for each sample.

Data were reduced using the commercially-available Iolite™ (V2.5; Paton et al., 2010) software package and the VizualAge data reduction scheme (Petrus and Kamber, 2012). Time resolved age, U/Th ratios, and isotopic signal intensities were interrogated for each measurement to identify issues such as Pb-loss, common Pb, age heterogeneities or measurements where the ablation pit exited the grain during measurement. Integration periods were modified to exclude regions of grains affected by these problems.

Uncertainty propagation was performed in a custom Excel™ VBA macro (ARS5.0)in accordance with community derived best-practices outlined in Horstwood et al. (2016) using the method of Matthews and Guest (2017). Standard deviations of the mean (s_m) were calculated as the standard deviation of all the indications of the isotopic ratio in the integration period, divided by the square root of the number of indications. Excess variance (ε)in the$^{206}Pb/^{238}U$ and $^{207}Pb/^{206}Pb$ ratios was calculated using a multi-sessional approach as outlined in Matthews and Guest (2016) and added quadratically to s_m to give the random data point uncertainty (s_x). Long-term excess variance (ε') was calculated using excess variance in validation reference materials 91500 ($^{206}Pb/^{238}U$) and 1242 ($^{207}Pb/^{206}Pb$). Systematic uncertainties associated with decay constants (λ), uncertainty in the ratios of the calibration reference material (s_y) and ε' were added in quadrature to yield the total uncertainty (S_{total}).

Data were filtered using the probability of concordance calculated by the concordia age algorithm in Isoplot 4.15 (Ludwig, 1998; Ludwig, 2012). Measurements with <1% probability of concordance were filtered from the dataset. Probability density functions were generated in DZStats (Saylor and Sundell, 2016) and are plotted using $^{206}Pb/^{238}U$ dates for grains younger than 1500 Ma and $^{207}Pb/^{206}Pb$ dates for grains older than 1500 Ma. All sources of random and systematic uncertainty were included in the plots.

Large-n (n = 660) Detrital Zircon Geochronology

All steps in the preparation of mounts, polishing, isotopic measurement, data reduction, filtering and data presentation are the same as for the n = 300 method with the

following modifications. To more efficiently collect the larger number of measurements the sample-standard bracketing procedure and ablation/background times were adjusted. Each measurement consisted of a 5 s ablation period and a 20 s gas blank was measured only during measurements of the calibration reference material. One measurement of the calibration reference material (FC1) was made between each 30 unknowns (approximately every 10 minutes). Up to 660 unknowns were measured per sample. Calibration of U and Th concentrations and validation reference materials the same as the n = 300 method. The short ablation time means that not enough of the grain is sampled to the evaluate whether factors such as grain isotopic homogeneity, Pb-loss or common Pb has compromised the measurement. As such, these data are useful for identifying grains for subsequent analysis, but individual grain dates are less reliable than for the n=300 measurement method. These data are still useful for population scale interpretations.

Lower Uncertainty Measurement Method

Near-depositional age grains, identified in the n = 300 and n = 660 datasets, were ablated at 7 Hz for 35 s using a 22 μm beam diameter. A 20 s gas blank was collected before each measurement. A signal smoothing manifold (Squid) was used to smooth out rapid changes in isotopic signal intensity (beating) which could occur at lower repetition rates (Müller et al., 2009). One measurement of the calibration reference material (Temora2; 416.78 Ma; Black et al., 2004) was made for each 4 to 5 measurements of the unknowns (approximately every 7 minutes). Eight measurements of each of three validation reference materials (Table 2) were used to validate the results.

Where possible, multiple ablations of each near-depositional age grain were used to assess for isotopic homogeneity and to improve the uncertainty of the final date (Spencer et al., 2016). Between one and four additional ablations were conducted on each grain. Dates for re-ablated grains were calculated using the weighted average $^{206}Pb/^{238}U$ and $^{207}Pb/^{206}Pb$ ratio of all re-ablations of the grain. Grains were deemed to be isotopically heterogeneous and were eliminated from the dataset if the MSWD of the weighted average ratio exceeded$1 + 2\sqrt{2/f}$where f is the degrees of freedom (n-1)(Wendt and Carl, 1991).

Calculation of Maximum Depositional Ages

Maximum depositional ages (MDA) were calculated using the results of the re-ablations. While it is possible to integrate the results of the detrital zircon dating (n = 300 and 660) into the MDA calculations, we see this as inadvisable due to differences in the crystallinity of the calibration reference material used for the detrital zircon measurements (FC1; low crystallinity) versus the re-ablations (Temora 2; moderate

crystallinity). This effect can result in systematic measurement errors of 1-2 % in the age of validation reference materials and unknowns (see Marillo-Sialer et al. (2016) for discussion) and might complicate the detection of Pb-loss or inheritance.Following the recommendations of Coutts et al. (2019) and Spencer et al. (2016) we used the weighted average $^{206}Pb/^{238}U$ age of the youngest multiply ablated grain (YMAG) as the MDA.

Results

Large n Detrital Zircon Results

Detrital zircon dating resulted in 1539 dates that passed our filtering criteria. Results are shown as frequency histograms and probability density functions (Figure 3). Complete isotopic data can be found in the supplementary tables. Both samples yielded similar detrital zircon populations regardless of the measurement method, albeit with somewhat different average grain uncertainty (2.3% for the 15 s ablations versus 4.2% for the 5 s ablations), so their results will be discussed together.

Yelverton samples yield detrital zircon populations characterized by diverse Mesoarchean to earliest Neoproterozoic zircon populations (Figure 3). Archean grains form a broad distribution of dates (4.0 to 2.5 Ga; modes ca. 2.72 Ga)and represent 30% of all measurements. Early Paleoproterozoic grains (2.5 to 2.0 Ga) are rare whereas late Paleoproterozoic grains (2.0 to 1.7 Ga; modes ca. 1.85 Ga) form the most common zircon population in the samples and represent 42% of all measurements. Mesoproterozoic grains (1.6 to 1.0 Ga; modes ca. 1.04 Ga) are common and are characterized by diverse modes.

Latest Neoproterozoic to Cambrian detrital zircon grains were found in both Yelverton samples but are rare, representing ~1% of the detrital zircon population (Figure 3). Individual grain dates range from late Ediacaran (567.9 ± 19.7 Ma) to mid-Cambrian (504.5 ± 21.5 Ma). All <600 Ma grains yield U/Th ratios <3.1 suggesting an igneous rather than metamorphic origin (Rubatto, 2017). The grains in this age fraction are rounded indicating that primary igneous sources had been eroded and that the grains were subject to sedimentary transport. One grain from an n = 660 ablation sequence yielded a Middle Ordovician (461.4 ± 16.5 Ma) date. However, a high uranium concentration in this grain (625 ppm) compared to other Ediacaran to Cambrian grains (average 245 ppm; Figure 4) leads us to suspect that the young date resulted from radiation damage induced Pb-loss (Mezger and Krogstad, 1997; Cherniak and Watson, 2000). Unfortunately, the grain was too small to re-ablate and it will not be considered further. A weighted average of all grains < 600 Ma (excluding the grain yielding an Ordovician date) yields an age of 531.9 ± 8.1 Ma (MSWD = 2.4)(Figure 5). The dates are over-dispersed indicating that either our analytical uncertainties are under-estimated, or the grains do not represent a single population (Wendt and Carl, 1991;

Spencer et al., 2016). It was not expected that there would have been a single igneous source because of the sedimentary character of the sample and rounded shape of the grains.

Re-Ablation Results

A total of 12 grains from the two samples were large enough to be re-ablated. Of these eight were large enough to fit more than one re-ablation. The $^{206}Pb/^{238}U$ ratios of three grains for which there were multiple re-ablations failed to adequately reproduce suggesting the grain was not isotopically homogenous due to either inheritance or Pb-loss. These grains will not be considered further. Results are presented as Wetherill concordia diagrams and weighted average plots (Figure 6). Full details of the isotopic measurements can be found in the supplementary tables.

Re-ablated grains yielded dates between Ediacaran (556.7 ± 17.3 Ma) and mid-Cambrian (518.2 ± 11.7 Ma). Interestingly, both the youngest and oldest grains in the re-ablation dataset were small grains where only a single re-ablation could be acquired. Considering only grains for which more than one re-ablation was obtained the range narrows to between 551.1 ± 8.9 Ma and 532.1 ± 9.1 Ma (Figure 6). All multiply ablated grains from 17-HSB-30-A1 overlap within uncertainty. The two multiply ablated grains from 17-HSB-31-A1 do not overlap suggesting they likely derive from different igneous sources.

Maximum Depositional Ages

Maximum depositional ages calculated for both samples are consistent and constrain the Yelverton to be no older than earliest Cambrian in age (Fortunian). Four concordant dates of the youngest multiply ablated grainin each of 17-HSB-30-A1 and 17-HSB-31-A1 yielded weighted average $^{206}Pb/^{238}U$ ages of 539.5 ± 7.6 Ma(MSWD 2.0) and 532.1 ± 9.1 Ma (MSWD 1.4), respectively. The large number of re-ablations (4), their good reproducibility (acceptable MSWD), and the internal consistency of the MDAs from both samples gives us high confidence in this result.

New constraints on the age of the Yelverton Formation

We use the U-Pb detrital zircon age data to inform the depositional age of the Yelverton Formation in two ways (incorporated into Fig. 2). First, of the two closely spaced samples, the youngest maximum depositional age provides information on how young the top of the Yelverton Formation is. The upper Yelverton Formation is younger than 532.1 ± 9.1 Ma (Early Cambrian) and is older than Early Cambrian trilobites from the Grantland Formation, which means that the top of the Yelverton Formation is Early Cambrian.

Secondly, the youngest U-Pb detrital zircon age probability peak in the Yelverton Formation is considered a proxy for the age of igneous rocks within the Yelverton Formation. This assumption is likely valid because: (1) the samples are from top of the formation and are stratigraphically above volcanic rocks of the Yelverton Formation; (2) the youngest part of the age peak overlaps with the depositional age of the Yelverton Formation; and (3) there are very limited igneous rocks of a similar age that are known from northern Ellesmere Island. Similar to the youngest age limit of detrital zircon, the oldest multiply ablated grain is 551.1 ± 8.9 Ma. A conservative estimate for the age of igneous rocks in the Yelverton Formation is therefore from 551.1 ± 8.9 Ma to 532.1 ± 9.1 Ma. This conservative age estimate is in contrast with the full range of single ablation U-Pb detrital zircon ages from the Lower Uncertainty Measurement Method which is 562.6 ±11.6 Ma to 518.2 ±10.0 Ma, which spans a larger age range.

Of course, these data are from a single outcrop locality and likely only provide a partial indication of the igneous rocks associated with the Yelverton Formation. There may be other igneous rocks in the Yelverton Formation with different ages, but data presented here can reliably attest to an age range of ca. 551-532 Ma.

Conclusion

The MDA for the uppermost Yelverton Formation is 532.1 ± 9.1 Ma. The age of the uppermost Yelverton Formation is therefore bracketed between this Early Cambrian MDA and previously reported Early Cambrian fossils (*Oldhamia*) from the Grantland Formation. The age range of igneous rocks within the Yelverton Formation is inferred from detrital zircon to be 551.1 ± 8.9 Ma to 532.1 ± 9.1 Ma.

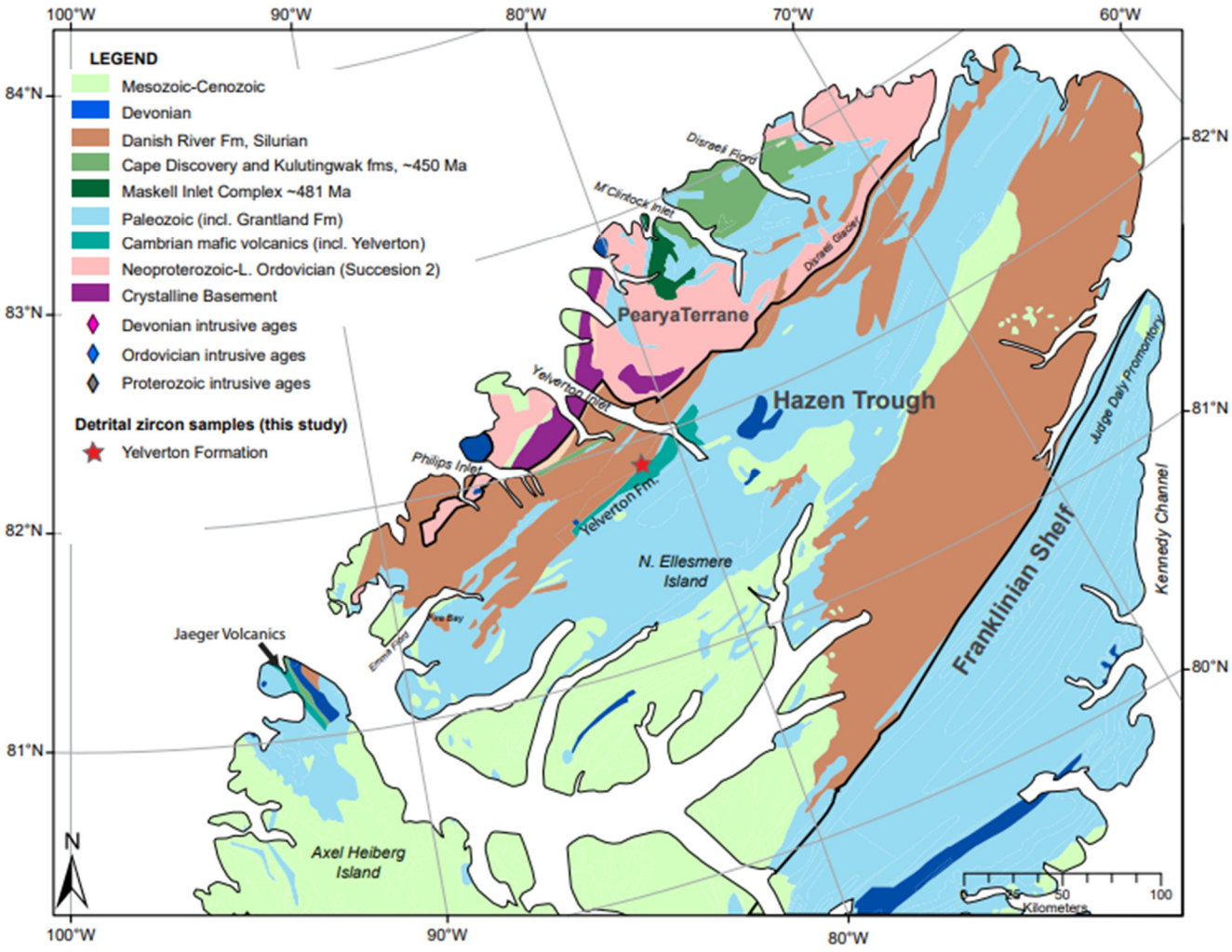

Figure 1: Map of Ellesmere Island. Geology from Okulitch (1991) is based on Trettin (1994, 1998).

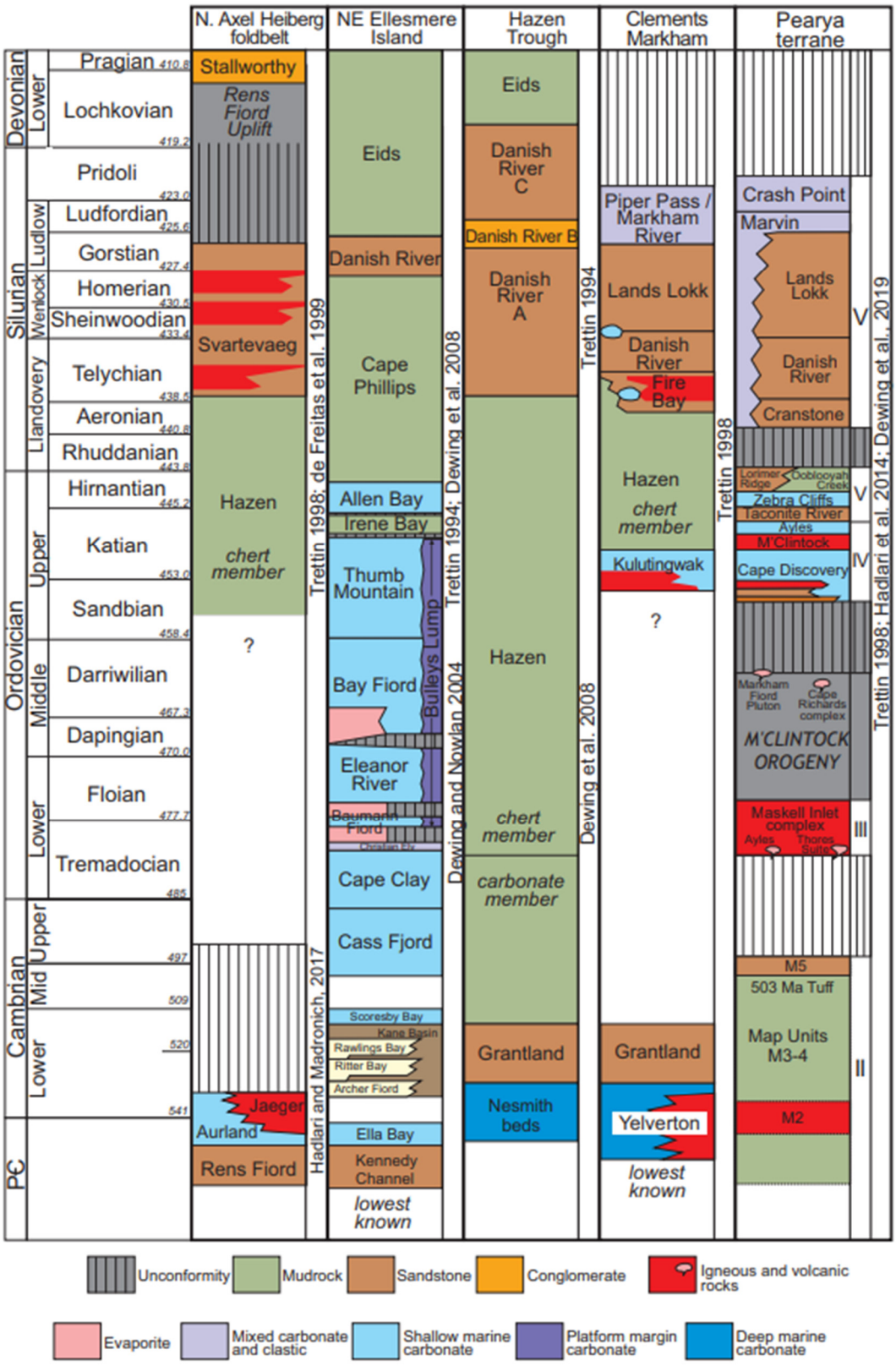

Figure 2: Stratigraphy of the Franklinian Basin from Trettin (1998) and Dewing et al. (2019), updated with an MDA for the Yelverton Formation of 532.1 ± 9.1 Ma.

Sample	Lithology	Stratigraphy	Lat.	Long.
17HSB030A01	sandstone	Yelverton Fm	81.8788	-81.5031
17HSB031A01	sandstone	Yelverton Fm	81.8781	-81.5038

Table 1: Sample location information.

Reference Material	Geological Unit	Age		Reference
		$^{206}Pb/^{238}U$	$^{207}Pb/^{206}Pb$	
FCT	Fish Canyon Tuff	28.201 ± 0.046	NA	Kuiper et al. (2008)
Temora 2	Middledale gabbroic complex	416.78 ± 0.33	NA	Black et al. (2011)
91500	Kuehl Lake, Ontario	1062.4 ± 0.4	1065.4 ± 0.3	Widenbeck et al. (1995, 2004)
FC-1	Duluth Anorthosite	1099.9 ± 1.1	1099.0 ± 0.6	Paces and Miller (1993
1242	Lac Frechette Syenite	2675.1 ± 1.1	2679.8 ± 0.2	Mortensen and Card (1993); Davis et al. (2019)

Table 2: Information pertaining to the calibration and validation reference materials used.

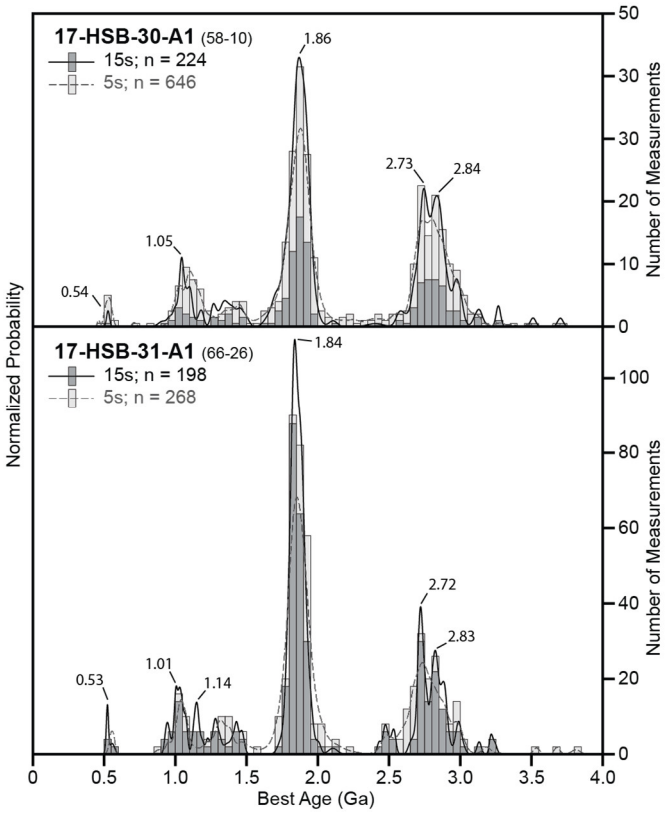

Figure 3: Normalized probability density functions and frequency histograms for 15 s and 5 s detrital zircon data; n is the number of measurements; the ages of significant modes are given in Ga.

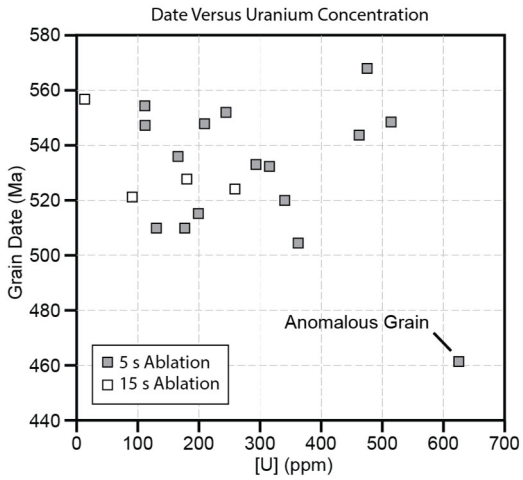

Figure 4: Grain date versus uranium concentration for all grains <600 Ma from both 15 s and 5 s detrital zircon datasets; grain that yielded anomalous Ordovician grain noted.

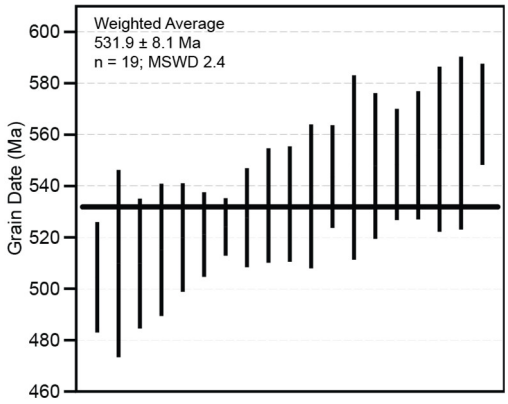

Figure 5: Ranked weighted average plot for<600 Ma grains from the 15 s and 5 s detrital zircon datasets; uncertainties are shows at 2σ.

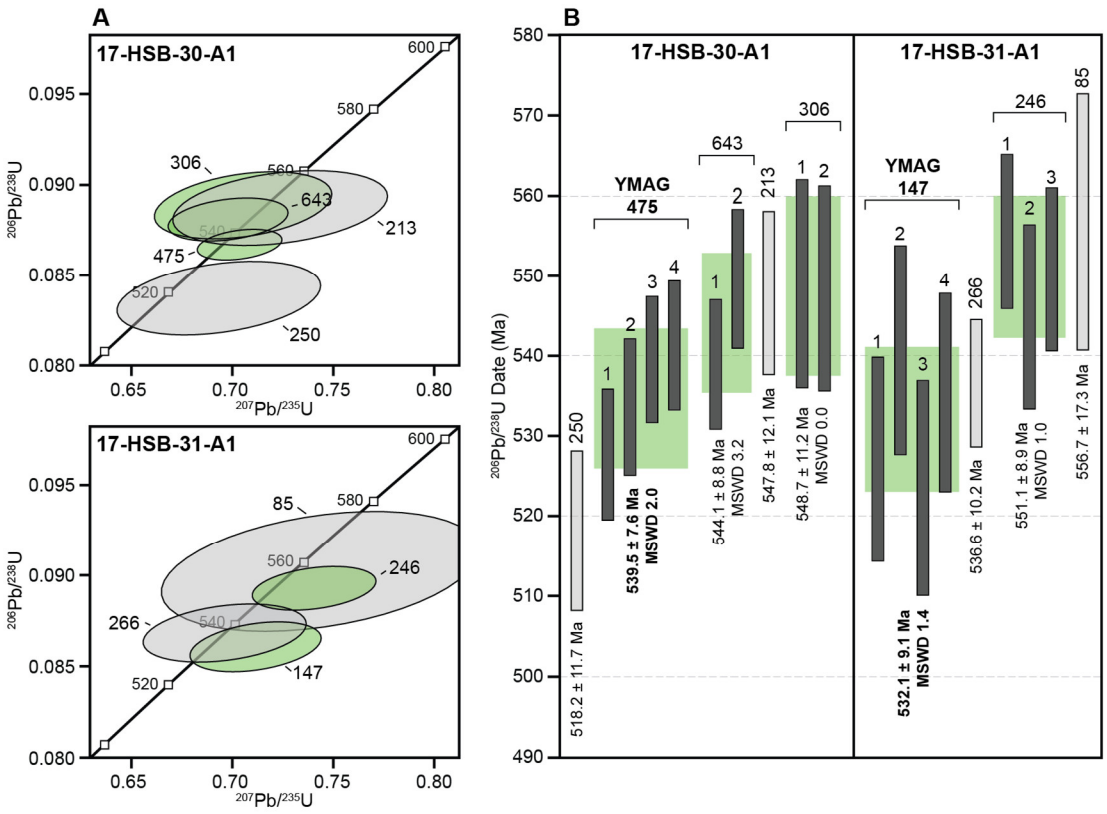

Figure 6: A) Wetherill Concordia diagram for re-ablations; grey ellipses are grains with only a single re-ablation; green ellipses are the weighted average of multiple ablations; ellipses are shown at 2σ uncertainty; numbers refer to the grain listed in supplementary datatable; B) weighted average plots for re-ablations; light grey bars are grains with only a single re-ablation; dark grey bars are individual measurements for grains with multiple ablations; green boxes are the weighted average $^{206}Pb/^{238}U$ ages for grains with multiple ablations; all uncertainties are reported at 2σ and include all random and systematic components (S_{total}).

References

Black, L.P., Kamo, S.L, Allen, C.M., Davis, D.W., Aleinkoff, J.N, Valley, J.W., Mundil, R., Campbell, I.H., Korsch, R.J., Williams, I.S., and Foudoulis, C., 2004. Improved 206Pb/238U microprobe geochronology by the monitoring of trace-element-related matrix effects; SHRIMP, ID-TIMS, ELA-ICP-MS and oxygen isotope documentation for a series of zircon standards; Chemical Geology, v. 205, p. 155-170.

Cherniak, D.J., Watson, E.B., 2000. Pb diffusion in zircon; Chemical Geology, v. 172, p. 5-24.

Cook, F.A., Coflin, K.C., Lane, L.S., Dietrich, J.R., and Dixon, J., 1987. Structure of the southeast margin of the Beaufort-Mackenzie basin, Arctic Canada, from crustal seismic-reflection data; Geology, v. 15, no. 10, p. 931-935. <https://doi.org/10.1130/0091-7613(1987)15<931:SOTSMO>2.0.CO;2>
doi:10.1130/0091-7613(1987)15<931:SOTSMO>2.0.CO;2

Coutts, D.S., Matthews, W.A., and Hubbard, S.M., 2019. Assessment of widely used methods to derive depositional ages from detrital zircon populations; Geoscience Frontiers, v. 10, p. 1421-1435.

Daniels, B.G., Auchter, N.C., Hubbard, S.M., Romans, B.Q., Matthews, W.A., andStright, L., 2017. Timing of deep-water slope evolution constrained by large-n detrital and volcanic ash zircon geochronology, Cretaceous Magallanes Basin, Chile; GSA Bulletin,v. 130, p. 438–454, doi: https://doi.org/10.1130/B31757.1

Davis, W.J., Pestaj, T., Rayner, N., and McNicoll, V.M., 2019. Long-term reproducibility of $^{207}Pb/^{206}Pb$ age at the GSC SHRIMP lab based on the GSC Archean Reference zircon z1242; Geological Survey of Canada, Scientific Presentations 111, 1 poster. https://doi.org/10.4095/321203

Dixon, J., Lane, L.S., Dietrich, J.R., McNeil, D.H., and Chen, Z., 2019. Chapter 17 - Geological History of the Late Cretaceous to Cenozoic Beaufort-Mackenzie Basin, Arctic Canada; in The Sedimentary Basins of the United States and Canada (Second Edition), (ed.) A.D. Miall; Elsevier, p. 695-717.

Horstwood M.S.A., Košler J., Gehrels G., Jackson S.E., McLean N.M., Paton C., Pearson N.J., Sircombe K., Sylvester P., Vermeesch P., Bowring J.F., Condon D.J. and Schoene B., 2016. Community-derived standards for LA-ICP-MS U-Th-Pb geochronology – uncertainty propagation, age interpretation and data reporting; Geostandards and Geoanalytical Research, v. 40, p. 311–332.

Kuiper, K.F., Deino, A., Hilgen, F.J., Krijgsman, W., Renne, P.R., and Wijbrans, J.R., 2008. Synchronizing rock clocks of Earth history. Science, v. 320, p. 500-504.

Ludwig K.R., 1998. On the treatment of concordant uranium-lead ages; Geochimica et Cosmochimica Acta, v. 62, p. 665–676.

Ludwig K.R., 2012. Isoplot v. 3.75 – A geochronological toolkit for Microsoft Excel. Berkeley Geochronology Center, Special Publication, v. 5, p. 1–75.

Marillo-Sialer, E., Woodhead, J., Hanchar, J.M., Reddy, S.M., Greig, A., Hergt, J., and Kohn, B., 2016. An investigation of the laser-induced zircon 'matrix effect'; Chemical Geology, v. 438, p. 11-24.

Matthews, W.A., and Guest, B., 2017. A practical approach to collecting large-n detrital zircon U-Pb data sets by quadrupole LA-ICP-MS; Geostandards and Geoanalytical Research, v. 41, p. 161-180.

Mezger, K., Krogstad, E.J., 1997. Interpretation of discordant UePb zircon ages: an evaluation; Journal of Metamorphic Geology, v. 15, p. 127-140.

Mortensen, J.K., and Card, K.D., 1993. U-Pb age constraints for the magmatic and tectonic evolution of the Pontiac Subprovince, Quebec; Canadian Journal of Earth Sciences, v. 30, p. 1970-1980.

Müller W., Shelley M., Miller P. and Broude S., 2009. Initial performance metrics of a new custom-designed AfF Excimer LA-ICP-MS system coupled to a two-volume laser-ablation cell; Journal of Analytical Atomic Spectrometry, v. 24, p. 209–214.

Paces, J.B., and Miller, J.D., 1993. Precise U-Pb ages of Duluth Complex and related mafic intrusion, Northeastern Minnesota: Geochronological insights to physical, petrogenetic, paleomagnetic, and tectonomagmatic processes associated with the 1.1 Ga Midcontinent Rift System; Journal of Geophysical Research, v. 98, p. 13997-14013.

Paton, C., Woodhead, J.D., Hellstrom, J.C., Hergt, J.M., Greig, A., and Maas, R., 2010. Improved laser ablation U-Pb zircon geochronology through robust downhole fractionation correction; Geochemistry Geophysics Geosystems, v. 11, p. 1-36.

Petrus, J.A., and Kamber, B.S., 2012.VizualAge: A novel approach to laser ablation ICP-MS U-Pb geochronology data reduction;Geostandards and Geoanalytical Research, v. 36, p. 247-270.

Rubatto, D., 2017. Zircon: the metamorphic mineral; Reviews in Mineralogy and Geochemistry, v. 83, p. 261-295.

Saylor, J.E., and Sundell, K.E., 2016. Quantifying comparison of large detrital geochronology data sets; Geosphere, v. 12, p. 1-18.

Spencer, C.J., Kirkland, C.L., and Taylor, R.J.M., 2016. Strategies towards statistically robust interpretations of in situ U-Pb zircon geochronology; Geoscience Frontiers, v. 7, p. 518-589.

Wendt, I., and Carl, C., 1991. The statistical distribution of the mean squared weighted deviation; Chemical Geology Isotope Geoscience Section, v. 86, p. 275-285.

Wiedenbeck, M., Alle, P., Corfu, F., Griffin, W.L. Meier, M., Oberli, F., Von Quadt, A., Roddick, J.C., and Spiegel, W., 1995. Three natural zircon standards for U-Th-Pb, Lu-Hf, trace element and REE analysis;Geostandards Newsletter, v. 19, p. 1-23.

Wiedenbeck, M., Hanchar, J.M., Peck, W.H., Sylvester, P., Valley, J., Whitehouse, M., Kronz, A., Morishita, Y., Nasdala, L., Fiebig, J., Franchi, I., Girard, J.P., Greenwood, R.C., Hinton, R., Kita, N., Mason, P.R.D., Norman, M., Ogasawara, M., Piccoli, P.M., Rhede, D., Satoh, H., Schulz-Dobrick, B., Skår, Ø., Spicuzza, M.J., Terada, K., Tindle, A., Togashi, S., Vennemann, T., Xie, Q., and Zheng, Y.F., 2004. Further characterisation of the 91500 zircon crystal; Geostandards and Geoanalytical Research, v. 28, p. 9-39.